Spermometer: electrical characterization of single boar sperm motility

Bjorn de Wagenaar, Ph.D.,[a] Daan J. Geijs, B.Sc.,[a] Hans de Boer,[a] Johan G. Bomer, B.Eng.,[a] Wouter Olthuis, Ph.D.,[a] Albert van den Berg, Ph.D.,[a] and Loes I. Segerink, Ph.D.[a,b]

[a] BIOS - Lab on a Chip Group, MESA+ Institute for Nanotechnology and MIRA Institute for Biomedical Technology and Technical Medicine, University of Twente, Enschede; and [b] Department of Obstetrics and Gynaecology, Radboud University Nijmegen Medical Centre, Nijmegen, the Netherlands

Objective: To study single sperm boar motility using electrical impedance measurements in a microfluidic system.
Design: Comparison of the optical data and electrical impedance data.
Setting: Research laboratory at a university.
Animal(s): Boar semen sample were used.
Intervention(s): A microfluidic system is developed that is able to spatially confine single boar sperm cells and allows noninvasive analysis of their motility on the single cell level. Using this system, the single sperm motility was affected by changing the temperature or adding chemical stimuli (caffeine). The retrieved electrical impedance and video data were processed using Matlab.
Main Outcome Measure(s): The sperm beat frequency and amplitude determined from the electrical impedance and video data.
Result(s): The electrically measured sperm beat frequency was verified by optical analysis and in correspondence. Furthermore the microfluidic platform allowed single sperm analysis by altering the sperm by temperature and chemical stimuli.
Conclusion(s): This platform could be exploited as a potential tool to study sperm cells on the single cell level and to perform advanced sperm selection for intracytoplasmic sperm injection (ICSI) applications. (Fertil Steril® 2016;106:773–80. ©2016 by American Society for Reproductive Medicine.)
Key Words: Microfluidic platform, cell trapping, sperm motility, impedance sensing, single sperm analysis

Discuss: You can discuss this article with its authors and with other ASRM members at https://www.fertstertdialog.com/users/16110-fertility-and-sterility/posts/10934-spermometer-electrical-characterization-of-single-boar-sperm-motility

In the past decennium (2000–2010) the amount of performed assisted reproduction treatments such as IVF and intracytoplasmic sperm injection (ICSI) has approximately doubled (1, 2). Especially, ICSI has won popularity for treatment of patients with no measurable sperm count (azoospermia) (3), but is also used in nonmale factor infertility cases, and has been performed >300,000 times in 2012 in Europe alone (4).

Sperm selection for ICSI treatments is based on visual inspection of the sperm. An important characteristic, which is used in the clinic for sperm selection, is the cell motility. At present, sperm selection for ICSI treatments is performed by manual inspection and selection of a motile sperm cell. Subsequently, a microneedle is used to isolate a single sperm cell, which is injected into an entrapped egg cell. This selection procedure can be subjective and time consuming, especially in cases of semen samples with a very low sperm count. Furthermore, a report of Ramos et al. (5) has shown that no more than 45% of the selected sperm cells for ICSI procedures have normal condensed nuclei. The ability of sperm cells to bind to hyaluronic acid is another mechanism that is reported to select mature sperm cells for ICSI (6, 7). Although the bounded sperm cells do not exhibit DNA fragmentation (6, 7), no improvement in pregnancy rates (PRs) and fertilization has been found using this technique as selection mechanism (8).

Selection of sperm cells with high motility using conventional (9) or microfluidic technologies (10, 11) have

Received February 25, 2016; revised and accepted May 12, 2016; published online June 6, 2016.
B.d.W. reports patent P100207EP00 pending. D.J.G. has nothing to disclose. H.d.B. has nothing to disclose. J.G.B. has nothing to disclose. W.O. has nothing to disclose. A.v.d.B. has nothing to disclose. L.I.S. reports grants from NWO Veni; semen samples provided by Topigs Norsvin; personal fees from Topigs Norsvin; STW Valorisation grant 2, outside the submitted work; and patents P100207EP00 and EP10170399.9 pending.
Supported by the NWO–Netherlands Organization of Scientific Research (Spinoza grant A.v.d.B., V.L.I.S.).
Reprint requests: Loes I. Segerink, Ph.D., Department of Obstetrics and Gynaecology, University of Twente, P.O. Box 217, Enschede 7500 AE, the Netherlands (E-mail: l.i.segerink@utwente.nl).

Fertility and Sterility® Vol. 106, No. 3, September 1, 2016 0015-0282/$36.00

http://dx.doi.org/10.1016/j.fertnstert.2016.05.008

shown higher DNA integrity compared with the unsorted semen sample. High sperm DNA integrity is important for successful fertilization, as a high degree of DNA fragmentation has shown a negative effect on ICSI outcome (12). Furthermore, the amount of DNA fragmentation in sperm has been inversely related to its potential to hyperactivate (13), which also elaborates on a potential relation between the sperm swimming behavior and DNA fragmentation. Although a variety of microfluidic systems have been developed for the selection of highly motile spermatozoa (10, 14–17), their application for single sperm selection for ICSI is limited.

Only a few reports have shown the capacity to manipulate and analyze sperm cells on the single cell level. Fuhr et al. (17) showed to ability to entrap motile sperm cells using electric field cages at frequencies in the megahertz range. Nascimento et al. (18) showed the potential to entrap single sperm cells using laser tweezers and to measure their motility optically. In previous work from our group, we used microcontact printed fibronectin spots to entrap single sperm cells, after which their motility was analyzed using image analysis (19). With a different approach, we used a hydrodynamic trapping procedure to entrap single sperm cells in small microfluidic channels to study their viability, acrosome integrity, and sex chromosome content using fluorescent analysis (20). These reports showed the ability to analyze single sperm motility and/or spatially confine single sperm cells. However, these reports all depend on optical analysis methods, which are controlled manually. A potential approach for automated analysis of single sperm cells is the combination of a trapping method with integrated microelectrodes for electrical analysis.

Therefore, we propose a microfluidic system that is capable of spatially confining single sperm cells and able to measure their motility electrically. This system could be a potential tool for advanced sperm analysis and selection for ICSI applications.

MATERIALS AND METHODS

Chip and Sample Preparation

The microfluidic setup consists of three parts: a polydimethylsiloxane (PDMS) chip with trapping features, a glass chip with microelectrodes, and a custom-made printed circuit board. Details on chip fabrication can be found in the Supplemental Material, available online. The microfluidic chip is illustrated in Figure 1A, containing all relevant channel and electrode dimensions. In Supplemental Figure 1 the alignment set-up needed for proper alignment of the electrodes and microfluidic channels is shown.

Before each experiment, the PDMS and glass surfaces were coated with poly(L-lysine)-grafted-poly(ethylene glycol) to prevent cell adhesion. The poly(L-lysine)-grafted-poly(ethylene glycol) was rinsed through the PDMS microchannels at a concentration of 100 μg/mL in deionized water for at least 15 minutes.

Fresh boar semen was obtained from a local artificial insemination centre ("KI Twenthe," Fleringen, the Netherlands) at a concentration of 20×10^6 cells/mL. The samples were diluted with Beltsville Thawing Solution (Solusem) to a concentration of 2×10^6 cells/mL. Boar sperm cells have the following dimensions: head length = ± 9 μm (21), head width = ± 4.5 μm (21), head volume = ± 12.5 fL (22), tail length = ± 45 μm (23).

Hydrodynamic Bead and Sperm Trapping

The hydrodynamic trapping procedure of sperm cells is described elsewhere (20). In short, 3- μm and 4-μm polystyrene beads (ø = 4.17 ± 0.03, ø = 2.9 ± 0.083, Polysciences

FIGURE 1

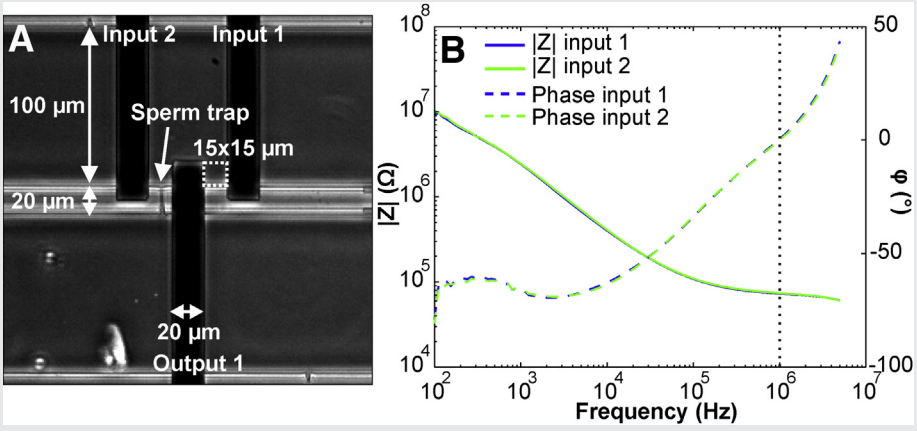

Microfluidic chip and electrical response. (**A**) The microfluidic chip consists of two main channels, interconnected by 2-μm wide and 1-μm high side channels, which act as cell traps. The electrode array consists of two sensing electrodes (input 1 and input 2) and one excitation electrode (output 1), which were used for differential impedance analysis. (**B**) The impedance and phase response of the microfluidic setup (without sperm cell) were investigated when sweeping frequency between 100 Hz and 5 MHz and recording under physiological conditions (σ_{el} = S/m) input 1 and input 2, separately.

de Wagenaar. Spermometer. Fertil Steril 2016.

Inc.) and sperm cells were trapped within the interconnecting channels between the two main channels of the PDMS chips. By generating a higher fluid flow in the bottom channel, compared with the flow in the bead-loaded or sperm-loaded top channel (0.025 and 5 μL/min, respectively), a fluid flow is created from the top to the bottom channel, which entrapped the beads or sperm cells. After trapping, the flow rate in the top channel was reduced to 0.01 μL/min.

Video Acquisition and Optical Data Analysis

Optical data was recorded using a Nikon TE2000-U microscope equipped with a ×10 phase contrast objective and a Basler acA780-75 camera at 75 fps. Analysis of the flagellar beat frequency was performed using a custom-built Matlab script. In short, this script is capable of tracking the sperm tail at a fixed vertical distance with respect to the channel wall. This position (i.e., X-location) is expressed with respect to the center of the two measurement electrodes. The interelectrode distance between these two electrodes is 15 μm and the X-location of the center is defined as 0 μm. After calibrating the optical data using the interelectrode distance (∼0.55 μm/pixel), the sperm tail is tracked between −7.5 and 7.5 μm. After plotting the position over time, frequency components within the signal were analyzed by performing a fast Fourier transform (FFT) to determine the flagellar beat frequency.

Differential Impedance Analysis and Data Analysis

The electrical impedance was recorded using an impedance spectroscope (HF2IS, Zurich Instruments) equipped with a preamplifier (HF2TA). A 1-MHz AC signal with an amplitude of 0.5 V was generated on output 1, which was connected to the exciting electrode of the electrode array (Supplemental Fig. 2A, available online). The two sensing electrodes were connected to input 1 and input 2 of the HF2IS by the HF2TA and used to measure the impedance, differentially (Supplemental Fig. 2B). Impedance was recorded using a bandwidth of 200 Hz and a sampling frequency of 899 Hz.

Recorded differential impedance data was imported and processed in Matlab (R2014b, MathWorks). The differential impedance response (Supplemental Fig. 2E) was obtained by subtracting the recorded impedance at input 1 (control, Supplemental Fig. 2C) from the impedance at input 2 (cell trap, Supplemental Fig. 2D). The FFT analysis was performed on the differential signal to calculate the sperm beat frequency. The amplitude of the motility-related oscillation was calculated after peak detection.

The impedance response of the microfluidic device as a function of frequency (100 Hz–5 MHz) was recorded simultaneously at input 1 and input 2 using a custom-built LabVIEW program.

RESULTS AND DISCUSSION

Platform Characterization

The microfluidic setup is illustrated in Figure 1A, consisting of three separate microelectrodes. A sinusoidal excitation is applied to the middle electrode, whereas the impedance is monitored simultaneously at the cell trap region and control region using electrodes connected to input 2 and input 1, respectively. This impedance is influenced by several components within the setup (Supplemental Fig. 2A): the electrode–electrolyte interface (C_{DL}), the electrolyte conductivity (R_{el}), and electrolyte capacitance (C_{el}). When introducing a sperm cell between the electrodes, the impedance is further influenced by the cell membrane and the cell interior. The electrical response of this setup (without sperm cell) was investigated by recording the impedance when sweeping the measurement frequency between 100 Hz and 5 MHz to find the optimal value for continuous impedance monitoring (Fig. 1B). A clear effect of C_{DL} was observed at the low frequency region (<100 kHz). At frequencies around 1 MHz, the absolute impedance was dominated by R_{el}, at which this impedance was around 100 kΩ and the phase shift was approximately 0. This frequency was selected for impedance monitoring in all reported experiments. The electrical response measured at both inputs showed almost identical behavior, indicating that the cell trap itself did not influence the electrical response of the setup. Therefore, the recorded impedance at input 1 is suitable as an internal control for differential measurement.

Bead and Sperm Trapping

Beads and sperm cells were captured by a hydrodynamic trapping procedure. By continuous impedance monitoring, the impedance change with bead and cell trapping was recorded. This change was determined after obtaining the differential impedance response. A typical trapping event of a 4-μm bead is shown in Supplemental Figure 3A, available online. The impedance change of 4-μm beads was 705 ± 10.7 Ω (mean ± SD, n = 10), whereas the impedance change of 3-μm beads was 210 ± 8.5 Ω (n = 10). When expressing the impedance change per volume of entrapped particle, the impedance changes for 3- μm and 4-μm beads were 16.4 Ω/μm^3 and 18.6 Ω/μm^3, respectively. For sperm cells, this value was approximately 26.2 Ω/μm^3. This value is significantly higher compared with those of the beads, which can be explained by the shape of the sperm cell. Due to the planar electrode geometry, the highest field strengths originate just above the glass substrate surface. Sperm cells have a flat shape and block the current to a bigger extend than the spherical beads.

Entrapment of sperm cells resulted in a head-first or tail-first capture of the cell (Supplemental Fig. 3B). At a measurement frequency of 1 MHz and in a high-conductive isotonic environment (1.4 S/m), the cell membrane acts as an insulator. As a result, the recorded impedance change increased with cell entrapment. To find out whether the orientation had an effect on the recorded impedance, the impedance change was determined for head-first and tail-first trapped sperm cells. The recorded impedance of 327 ± 73 Ω (n = 25) and 319 ± 59 Ω (n = 25), respectively, showed no difference between the two orientations.

Sperm cells have a natural tendency to swim close to surfaces and to swim against small fluid flows (16, 24, 25). This behavior was also observed in our microfluidic system (results not shown). As a result, trapping sperm cells head-first was rather straightforward, because the sperm heads were

positioned in close distance to the cell traps when swimming. With sperm entrapment, the recorded impedance data showed an initial increase as previously shown (Supplemental Fig. 3B). Interestingly, after cell trapping, a repetitive oscillation in the differential impedance was observed with more amplitude compared with the recorded noise (Fig. 2A and Supplemental Video 1). This oscillation was caused by the motile behavior of the sperm cell.

Entrapped sperm cells showed good cell motility during periods exceeding 15 minutes, which points to the noninvasive nature of the trap and analysis techniques. However, when the sperm head came in direct contact with one of the electrodes, the motility was observed to decline or the sperm cell was temporarily paralyzed (data not shown). This finding, combined with the simulated field strength (SI text) of >500 V/cm close to the excitation electrode (Supplemental Fig. 4, available online), are consistent with the observations by Fuhr et al. (17), describing sperm immobilization at field strengths of around 500 V/cm. Although this suggests that the functioning of the cells is not harmed when they are not in contact with the electrodes, it does not guarantee that other properties of the cell are not affected. Therefore before this technique can be finally used in the clinic, studies on the noninvasiveness of the platform needs to be carried out.

Optical and Electrical Analysis of Sperm Motility

To investigate whether the recorded impedance provides information on sperm motility as previously described, the flagellar motion of a trapped cell between the electrodes was recorded optically at a frame rate of 75 fps (Supplemental Video 2, n = 1). Subsequently, a custom-made Matlab program was used to automatically track the sperm tail at a fixed height (C).

This position, expressed as an X-location with respect to the electrode array's center, described a motion along the X-axis (Supplemental Fig. 5 and Fig. 2B). When comparing the obtained optical data (Fig. 2C) with the electrical data (Fig. 2D) the oscillation in the optical data and the electrical data showed a similar frequency. After performing a FFT, an identical base frequency was found (Fig. 2E) which was around 14.5 Hz for this particular cell. This base frequency, which is related to the sperm motility, is called the sperm beat frequency.

In literature, the sperm beat cross frequency (BCF) is a parameter that is defined as the frequency of the sperm head crossing the sperm average path (26, 27), expressed as the amount of intersections (in either direction) per second (in hertz). In our reported experiments, the obtained frequency represents the amount of tail oscillations per second, in which a single oscillation is defined as the movement of the sperm tail from the first electrode toward the second electrode and back. In this case, in a single oscillation the sperm cell crosses its hypothetical path (i.e., center line) twice. Therefore, the BCF of the entrapped sperm cell (n = 1) is determined by multiplying the calculated beat frequency by a factor of 2, yielding a BCF of approximately 29 Hz for this particular case. This result is comparable with the average BCF of 31.5 Hz of a control sample, which was determined by Computer Assisted Semen Analysis (CASA) analysis (SI text, n = 220).

Temperature-dependent Sperm Motility

To distinguish between sperm cells with a high or low motility, the electrical analysis technique should be able to quantify the swimming behavior of sperm cells with varying motility. As a model system, we used an entrapped sperm cell and decreased the temperature to mimic sperm cells with a reduced motility. Subsequently, the temperature was increased to observe the recovery of sperm motility.

After entrapping a sperm cell, the hot-plate was switched off (t = 0 seconds). At 5 minutes, the hot-plate was switched on again and data were recorded up to 10 minutes. The differential impedance data were used to construct a FFT spectrum every 5 seconds. At t = 0 seconds, a frequency around 35 Hz was observed in the FFT spectrum. As the temperature decreased over time, a clear left shift of the base frequency was observed in the spectrum (Supplemental Fig. 6A, available online, and Supplemental Video 3, n = 1). After 5 minutes, the motility reduced to frequencies around 15 Hz. When the temperature started to increase after switching on the hot-plate, the measured frequency clearly shifted to the right. After 10 minutes, the flagellar frequency recovered to a value between 30 and 35 Hz (Supplemental Fig. 6B and Supplemental Video 3, n = 1). This beat frequency was significantly higher compared with the beat frequency shown in Fig. 2E determined from a different trapped sperm cell (n = 1). This difference is likely caused by differences in intrinsic sperm motility between the two entrapped cells.

A data fit were constructed for each separate FFT spectrum and the maximum of this fit was determined, which represents the average flagellar beat frequency. This average frequency was plotted over time to show the declining and ascending trends in frequency (Fig. 3A, n = 1). Furthermore, the temperature on the surface of the glass chip was measured (SI text) to show the trend in temperature (n = 1). The frequency was observed to gradually decrease over time in a roughly linear fashion (Fig. 3A). After switching on the hot-plate, the temperature was observed to increased, and interestingly, the beat frequency increased accordingly. When considering a delay between the temperature of the glass (measured) and the temperature of the fluid in the microchannel (unknown), a good correspondence was found between the trends in temperature and sperm beat frequency (Fig. 3B).

Chemical Stimulation

Various factors are known to influence sperm motility besides temperature, including the internal pH and calcium concentration (28, 29). Furthermore, several chemical compounds are known to alter the swimming behavior of sperm including P (30), caffeine (31), and calcium ionophore A23187 (32). To show the effect of chemical stimulation on single sperm motility and to investigate whether this effect can be measured electrically, trapped sperm cells were exposed to caffeine (SI text). Moderate intake of caffeine did not show an effect on the sperm motility in a human

FIGURE 2

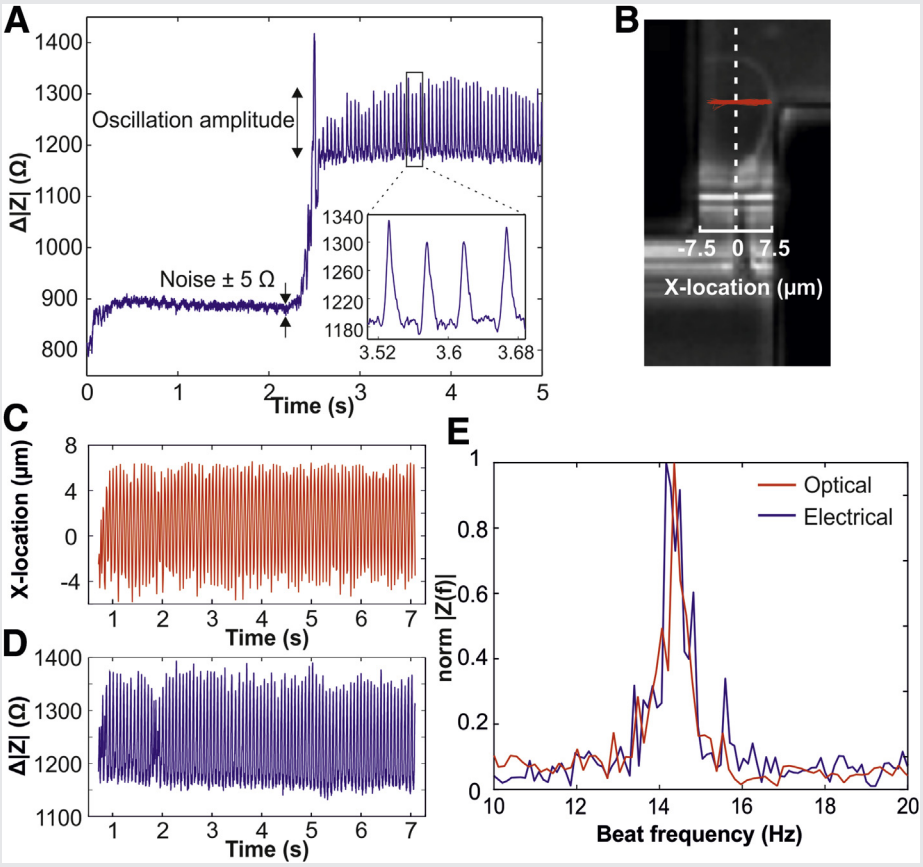

Optical and electrical analysis of single sperm motility, (**A**) Recorded impedance before and after trapping of a motile sperm cell. After cell trapping, the impedance increased with approximately 300 Ω and a steady oscillation was observed in the impedance response, which was caused by to the motile behavior of the spermatozoon. (**B**) The sperm flagellum of an entrapped sperm cell was tracked using a custom-build Matlab program. (**C**) When plotting the position of the tail (X-position) over time, an oscillation was observed that was comparable to (**D**) the electrical response. (**E**) Fast Fourier transform analysis of both optical and electrical data showed an identical base frequency at approximately 14.5 Hz.

de Wagenaar. Spermometer. Fertil Steril 2016.

population (33); however, direct exposure to this compound in vitro is known to increase sperm motility (31).

After trapping a sperm cell head-first, 4 mM of caffeine was added to the channel insert, yielding a final concentration of ±2 mM. Before adding caffeine, the sperm cell showed a stable beat frequency at approximately 15 Hz (Fig. 3C, n = 1). After adding the caffeine, the frequency did not change instantly. However, after an additional 30 seconds, the beat frequency was observed to increase gradually to a maximum of 22 Hz. This offset is probably caused by a delay between caffeine insertion and cell exposure due to a low flow rate in the cell-containing channel.

Interestingly, the total amplitude of the signal decreased over time. After cell entrapment, the signal amplitude was approximately 250 Ω, whereas this value decreased to less than 150 Ω at the end of the experiment. Possibly this decrease is related to the decline in flagellar beat angle (FBA). When the beat frequency of the cell increased, the angle of the beating flagellum decreased simultaneously (optically verified; results not shown). Correspondingly, the total displacement of the sperm head with respect to the X-axis started to decrease over time (i.e., the distance between the sperm head and the edges of the electrodes started to increase). As a result, the signal amplitude decreased. In a second experiment, similar effects on the beat frequency and the motility-related signal amplitude were observed by exposing an entrapped sperm cell to caffeine (Fig. 3D). At the start of the experiment, a frequency of 20–21 Hz and a signal amplitude of ±475 Ω were recorded. This frequency increased to a maximum of 28–29 Hz and the amplitude decreased to values <400 Ω after caffeine exposure (Fig. 3D). These preliminary data showed a potential relation between FBA and the amplitude of the motility-related oscillation. Using this platform, the effect of a chemical stimulus on the beat frequency of a single sperm cell was investigated.

Hyperactivation

Hyperactivation is an important phenomenon that aids the sperm cell to migrate to and penetrate the zona pellucida

FIGURE 3

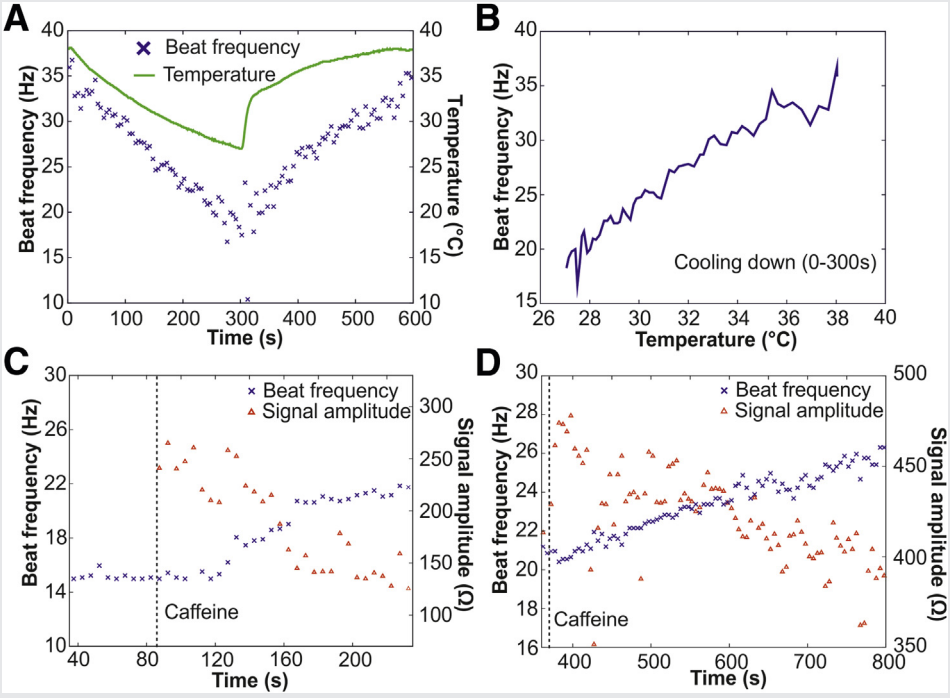

The effect of temperature and chemical stimuli on sperm beat frequency. (**A**) Fast Fourier transform analysis was performed at a 5-second interval when decreasing and increasing the fluid temperature. The sperm beat frequency was observed to decrease when the solution was cooling down. Correspondingly, the sperm beat frequency increase with temperature increase. (**B**) The relation between base frequency and temperature showed a linear behavior (when cooling down). (**C**) After cell entrapment at 35 seconds, a steady beat frequency was observed of approximately 15 Hz. After introducing caffeine at 86 seconds, a steady increase of the beat frequency to approximately 22 Hz was observed, starting at 120 seconds. correspondingly, the oscillation amplitude was observed to decrease. (**D**) For a second sperm cell, a similar effect was observed on the beat frequency and oscillation amplitude. After cell entrapment (360 seconds) and caffeine exposure (370 seconds), the beat frequency was observed to increase from 20–21 Hz to 28–29 Hz. The amplitude of the oscillation was observed to decrease over time from 450–500 Ω to values between 150 and 200 Ω.

de Wagenaar. Spermometer. Fertil Steril 2016.

(ZP) of the egg cell. During hyperactivation, sperm cells show an asymmetric beat pattern with increased flagellar amplitude. Research has shown a decrease in hyperactivation potential with an increase of DNA fragmentation (13). Because DNA fragmentation has shown a negative effect on ICSI outcome (12), the potential to distinguish and select hyperactivated sperm cells from nonhyperactivated sperm cells could provide useful information for advanced sperm selection.

Hyperactivated motility is characterized by asymmetric tail beating, in which the FBA is increased and the flagellar beat frequency is decreased (32, 34). Previous results have shown the potential to investigate the beat frequency. Furthermore, exposure to caffeine resulted in increased sperm beat frequency and decreased signal amplitude, which was likely caused by a decrease in beat angle. To investigate the potential to electrically distinguish between nonhyperactivated and hyperactivated sperm cells, the FBA, frequency, and signal amplitude were measured of sperm cells with distinct swimming behavior on a single chip.

In most occasions, sperm cells showed symmetrical tail beating before entrapment, which swam close to the channel wall. An example is shown in Fig. 4A. During entrapment, a FBA of 59° ± 11° (Fig. 4A, n = 1) and a BCF of 36 Hz (Fig. 4B, n = 1) were measured. These data are consistent for a sperm cell that is nonhyperactivated (34).

In a rarer occasion, a sperm cell was trapped, which showed asymmetrical tail beating, pushing the cell away from the channel wall (Supplemental Video 4). After entrapment, the sperm cell showed hyperactivated behavior with an increased FBA of 93° ± 11° (Fig. 4C, n = 1) and a decreased BCF of 24 Hz (Fig. 4D, n = 1). The signal amplitude of the hyperactive sperm cell (522 ± 16 Ω) was significantly higher compared with the amplitude (190 ± 15 Ω) of the nonhyperactivated sperm cell (Supplemental Video 5). This increase is in agreement with the increase of FBA of a hyperactivated sperm cell.

The observed increase in amplitude can be explained by the position of the sperm head with respect to the electrodes and the resulting electrical field. As expected, the electrical field is not uniform due to the geometry of the electrode array (Supplemental Fig. 4A). When illustrating the normalized electrical field strength in between the electrodes at the opposite sides of the trapping site (Supplemental Fig. 4B), the field strength was approximately two times higher close to the

FIGURE 4

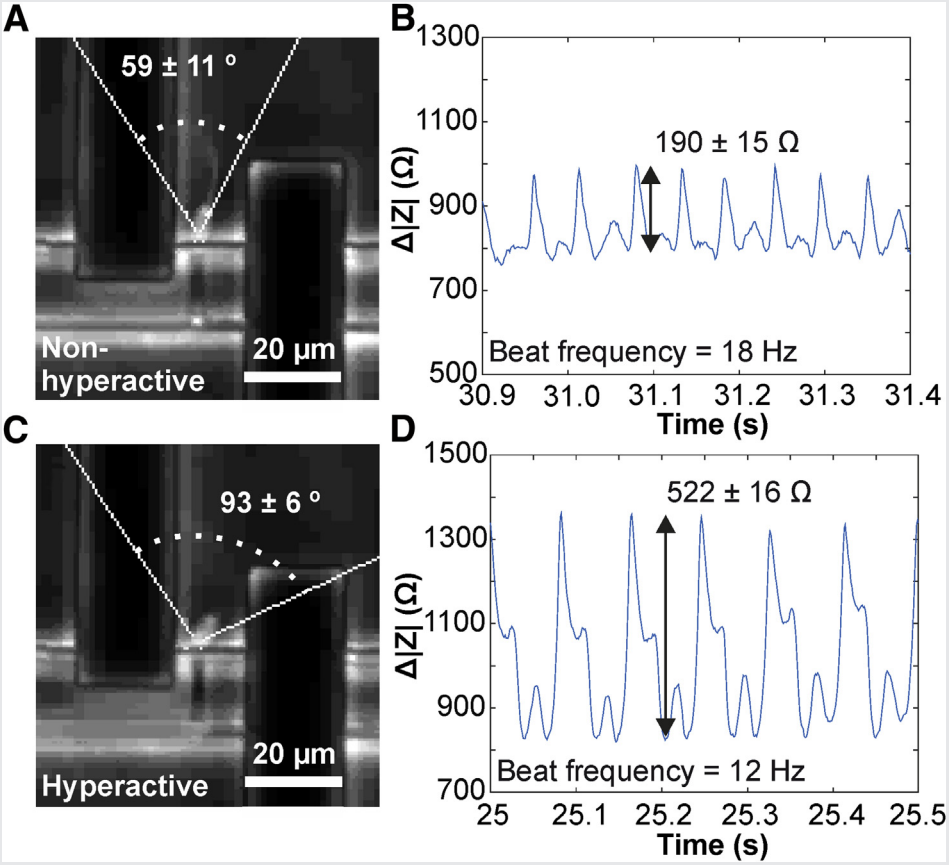

Hyperactivation of sperm. In two separate experiments, two sperm cells were entrapped, in which one of them was hyperactivated. The beat frequency, flagellar beat angle, and oscillation amplitude were investigated during a fixed interval of 0.5 seconds. (**A** & **C**) The flagellar beat angle of a hyperactive sperm cell was higher compared with a nonhyperactive spermatozoon (59° ± 11° and 93° ± 6°, respectively). (**B** & **D**) Correspondingly, the beat frequency was smaller for the hyperactivated sperm cell (12 Hz compared to 18 Hz). As a result of smaller flagellar beat angle, the recorded oscillation amplitude of the hyperactivated sperm cell was higher compared with the nonhyperactived sperm cell (522 ± 16 Ω and 190 ± 15 Ω, respectively).

de Wagenaar. Spermometer. Fertil Steril 2016.

exciting electrode (x = 15 μm) than at the sensing electrode (x = 0 μm). As a consequence, sperm movement toward the exciting electrode will result in a higher change in impedance compared with movement toward the sensing electrode. This finding is consistent with the observed results.

In conclusion, we characterized and developed a microfluidic platform for the entrapment of single sperm cells and the electrical analysis of single sperm motility. The sperm flagellar beat frequency was characterized by electrical impedance monitoring, which was verified by optical tracking of the sperm flagellum. Using electrical analysis, the effect of temperature alteration and caffeine exposure was observed on the sperm beat frequency. A clear difference in beat frequency and FBA was observed between nonhyperactivated and hyperactivated sperm cells.

The potential to select sperm cells individually based on swimming behavior holds promise for improved sperm selection for ICSI treatments. For this we envision that in our microfluidic system all the available sperm cells present will be trapped and analyzed such that the best ones can be selected. The current layout is not very suitable for use in the clinic as it is difficult to retrieve a single sperm. One can think of a different layout where the trapping channels envelop an open, circular well in which a sample is introduced. Because this well is open, one can easily retrieve a single sperm by using a microneedle. Subsequently, additional sample processing could be needed as in most cases the sperm have poor quality and low concentration. An innovative filtration step might be a solution for micro-testicular sperm extraction (TESE) samples or other azoospermic samples to retrieve all the available sperm cells yet removing most of the debris and other cells. Such a step can be integrated in the microfluidic platform such that an integrated platform exists for this application. Furthermore, the presented platform could be exploited to study sperm processes like maturation, hyperactivation, and chemotaxis on the single cell level.

Acknowledgments: The scientific support of Jean-Philippe Frimat, C.C.L. Denoeud, and Jorien T.W. Berendsen and the technical support of Paul M. ter Braak and Jan van

Nieuwkasteele are gratefully acknowledged. The authors also thank the "KI Twenthe" for the kind supply of boar semen samples.

REFERENCES

1. Kupka MS, Ferraretti AP, de Mouzon J, Erb K, Castilla JA, Calhaz-Jorge C, et al. Assisted reproductive technology in Europe, 2010: results generated from European registers by ESHRE. Hum Reprod 2014;29:2099–113.
2. Nyboe Andersen A, Gianaroli L, Nygren KG. Assisted reproductive technology in Europe, 2000. Results generated from European registers by ESHRE. Hum Reprod 2004;19:490–503.
3. Boulet SL, Metha A, Kissin DM, Warner L, Kawwass F, Jamieson DJ. Trends in use of and reproductive outcomes associated with intracytoplasmic sperm injection. JAMA 2015;313:255–63.
4. Kupka M, Calhaz-Jorge C, Castilla Alcala JA, de Geyter C, de Mouzon J, D'Hooghe T, et al. Assisted reproductive technology (ART) in Europe 2012. Preliminary results generated from European registers by ESHRE. ESHRE Annual meeting. June 14-17, Lisbon, Portugal 2015.
5. Ramos L, de Boer P, Meuleman EJH, Braat DDM, Wetzels AMM. Evaluation of ICSI-Selected epididymal sperm samples of obstructive azoospermic males by the CKIA system. J Androl 2004;25:406–11.
6. Huszar G, Ozkavukcu S, Jakab A, Celik-Ozenci C, Sati GL, Cayli S. Hyaluronic acid binding ability of human sperm reflects cellular maturity and fertilizing potential: selection of sperm for intracytoplasmic sperm injection. Curr Opin Obstet Gynecol 2006;18:260–7.
7. Huszar G, Jakab A, Sakkas D, Ozenci CC, Cayli S, Delpiano E, et al. Fertility testing and ICSI sperm selection by hyaluronic acid binding: clinical and genetic aspects. RBM Online 2007;14:650–63.
8. Beck-Fruchter R, Shalev E, Weiss A. Clinical benefit using sperm hyaluronic acid binding technique in ICSI cycles: a systematic review and meta-analysis. RBM Online 2016;32:286–98.
9. Jackson RE, Bormann CL, Hassun PA, Rocha AM, Motta ELA, Serafini PC, et al. Effects of semen storage and separation techniques on sperm DNA fragmentation. Fertil Steril 2010;94:2626–30.
10. Nosrati R, Vollmer M, Eamer L, San Gabriel MC, Zeidan K, Zini A, et al. Rapid selection of sperm with high DNA integrity. Lab Chip 2014;14:1142–50.
11. Zhang B, Yin TL, Yang J. A novel microfluidic device for selecting human sperm to increase the proportion of morphologically normal, motile sperm with uncompromised DNA integrity. Anal Methods 2015;7:5981–8.
12. Benchaib M, Braun V, Lornage J, Hadj S, Salle B, Lejeune H, et al. Sperm DNA fragmentation decreases the pregnancy rate in an assisted reproductive technique. Hum Reprod 2003;18:1023–8.
13. Chan PJ, Corselli JU, Patton WC, Jacobson JD, Chan SR, King A. A simple comet assay for archived sperm correlates DNA fragmentation to reduced hyperactivation and penetration of zona-free hamster oocytes. Fertil Steril 2001;75:186–92.
14. Tasoglu S, Safaee H, Zhang X, Kingsley JL, Catalano PN, Gurkan UA, et al. Exhaustion of racing sperm in nature-mimicking microfluidic channels during sorting. Small 2013;9:3374–84.
15. Cho BS, Schuster TG, Zhu X, Chang C, Smith GD, Takayama S. Passively driven integrated microfluidic system for separation of motile sperm. Anal Chem 2003;75:1671–5.
16. Duck-bong S, Agca Y, Feng ZC, Critser J. Development of sorting, aligning, and orienting motile sperm using microfluidic device operated by hydrostatic pressure. Microfluid Nanofluid 2007;3:561–70.
17. Fuhr G, Müller T, Baukloh V, Lucas K. High-frequency electric field trapping of individual human spermatozoa. Hum Reprod 1998;13:136–41.
18. Nascimento JL, Botvinick EL, Shi LZ, Durrant B, Berns MW. Analysis of sperm motility using optical tweezers. J Biomed Opt 2006;11:044001–8.
19. Frimat JP, Bronkhorst M, de Wagenaar B, Bomer JG, van der Heijden F, van den Berg A, et al. Make it spin: individual trapping of sperm for analysis and recovery using micro-contact printing. Lab Chip 2014;14:2635–41.
20. De Wagenaar B, Berendsen JT, Bomer JG, Olthuis W, van den Berg A, Segerink LI. Microfluidic single sperm entrapment and analysis. Lab Chip 2015;15:1294–301.
21. Saravia F, Núñez-Martínez I, Móran JM, Soler C, Muriel A, Rodríguez-Martínez H, et al. Differences in boar sperm head shape and dimensions recorded by computer-assisted sperm morphometry are not related to chromatin integrity. Theriogenology 2007;68:196–203.
22. Petrunkina AM, Hebel M, Waberski D, Weitze KF, Topfer-Petersen E. Requirement for an intact cytoskeleton for volume regulation in boar spermatozoa. Reproduction 2004;127:105–15.
23. Kondracki S, Iwanina M, Wysokinska A, Huszno M. Comparative analysis of Duroc and Pietrain boar sperm morphology. Acta Vet Brno 2012;81:195–9.
24. Qiu T, Han C, Ma R, Xie L, Li Z, Su K, et al. A microfluidic "treadmill" for sperm selective trapping according to motility classification. Solid-State Sensors, Actuators and Microsystems Conference (TRANSDUCERS), Bejing, 2011 16th International:1320–1323.
25. Lopez-Garcia MD, Monson RL, Haubert K, Wheeler MB, Beebe DJ. Sperm motion in a microfluidic fertilization device. Biomed Microdevices 2008;10:709–18.
26. Mortimer D. Practical laboratory andrology. New York: Oxford University Press; 1994.
27. McQueen CA. Comprehensive toxicology. 2nd ed. Amsterdam: Elsevier Ltd.; 2010.
28. Gatti J-L, Chevrier C, Paquignon M, Dacheux J-L. External ionic conditions, internal pH and motility of ram and boar spermatozoa. J Reprod Fertil 1993;98:439–49.
29. Satake N, Elliott RM, Watson PF, Holt WV. Sperm selection and competition in pigs may be mediated by the differential motility activation and suppression of sperm subpopulations within the oviduct. J Exp Biol 2006;209:1560–72.
30. Barboni B, Mattioli M, Seren E. Influence of progesterone on boar sperm capacitation. J Endocrinol 1995;144:13–8.
31. Peláez J, Breininger E, Alegre B, Peña FJ, Domínguez JC. In vitro evaluation of the quality and fertilizing capacity of boar semen frozen in 0.25 ml straws. Reprod Domest Anim 2006;41:153–61.
32. Schmidt H, Kamp G. Induced hyperactivity in boar spermatozoa and its evaluation by computer-assisted sperm analysis. Reproduction 2004;128:171–9.
33. Jensen TK, Swan SH, Skakkebæk NE, Rasmussen S, Jørgensen N. Caffeine Intake and Semen Quality in a Population of 2,554 Young Danish Men. Am Journal of Epidemiol 2010;171:883–91.
34. Mortimer ST, Schoevaert D, Swan MA, Mortimer D. Quantitative observations of flagellar motility of capacitating human spermatozoa. Hum Reprod 1997;12:1006–12.

SUPPLEMENTAL FIGURE 1

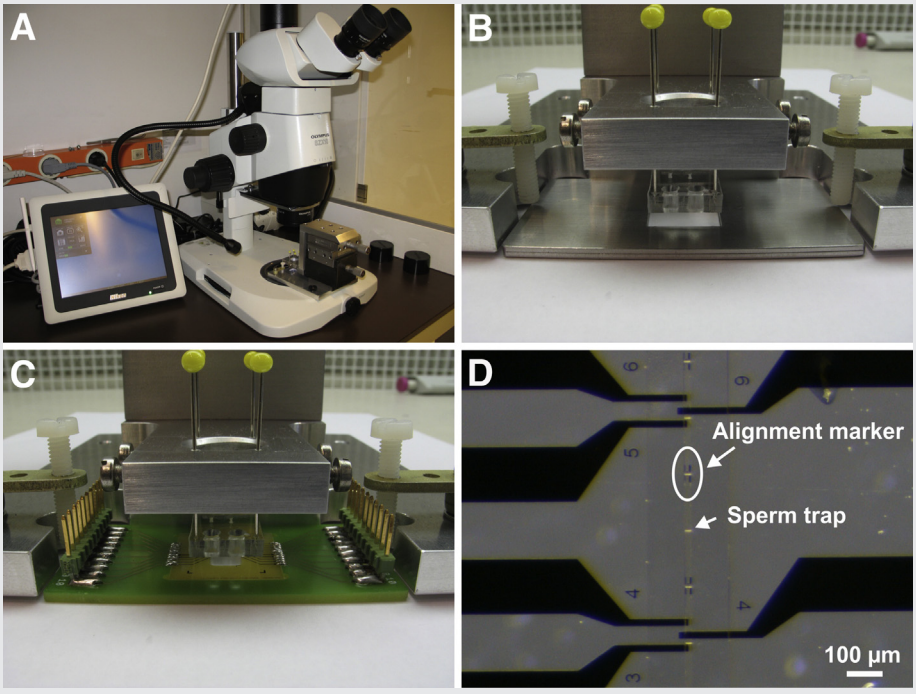

Alignment setup for polydimethylsiloxane and glass chips. (**A**) Using a stereo microscope and (**B**) an adapted XYZ-table (**B** & **C**), polydimethylsiloxane chips were picked-up with a needle array and (**D**) aligned to the microelectrodes on the glass chips using special alignment markers on the glass chips.

de Wagenaar. Spermometer. Fertil Steril 2016.

SUPPLEMENTAL FIGURE 2

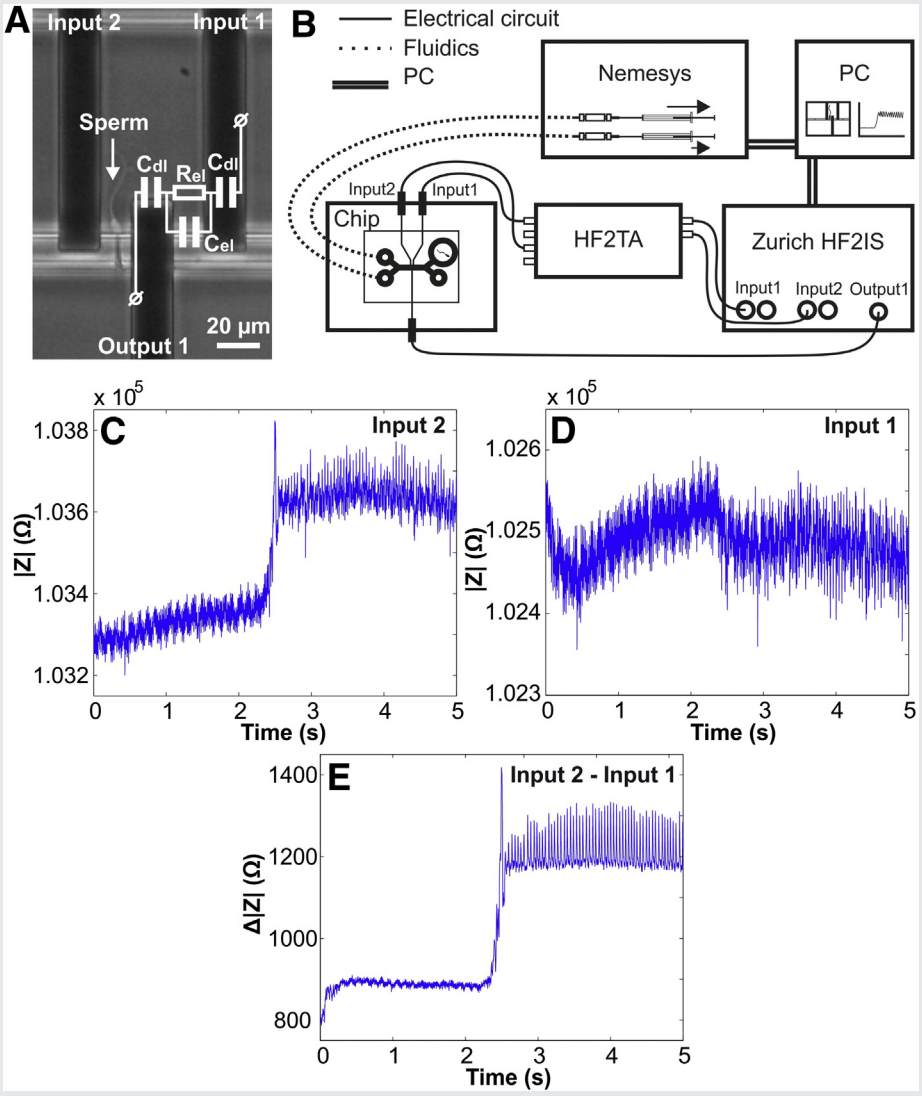

Electrical analysis of single sperm motility. (**A**) Microfluidic chip including equivalent circuit model for an empty trap. (**B**) Illustration of the electrical setup. The microelectrodes for data recording are connected to input 1 and input 2 of the impedance spectroscope through the preamplifier; a sinusoidal excitation is applied to the microelectrode connected to output 1. (**C**) The recorded impedance at input 1 (**D**) the impedance recorded at input 2 (**E**) the differential impedance response obtained by subtracting input 2 from input 1.

de Wagenaar. Spermometer. Fertil Steril 2016.

SUPPLEMENTAL FIGURE 3

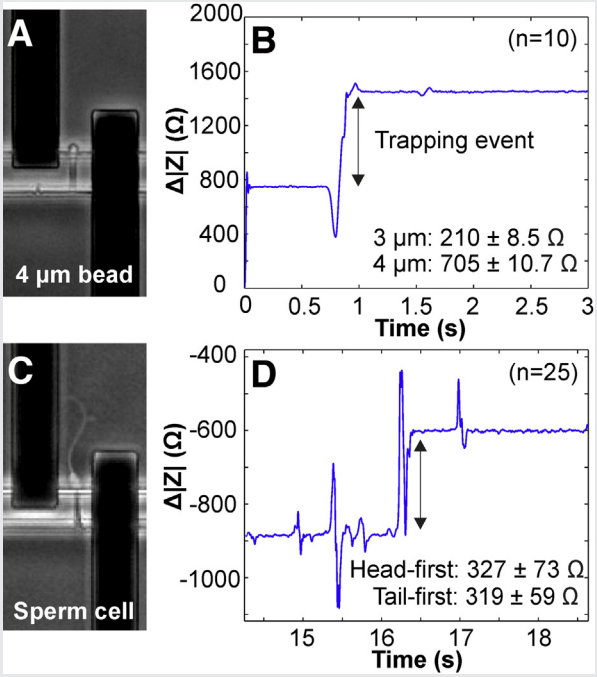

(**A**) Microscopic image of a trapped bead and (**B**) Recorded impedance change with trapping of 3-μm or 4-μm beads (n = 10) (**C**) Microscopic image of a trapped sperm cell and (**D**) sperm cells in head-first or tail-first orientation (n = 25). Values are reported in mean ± SD.

de Wagenaar. Spermometer. Fertil Steril 2016.

SUPPLEMENTAL FIGURE 4

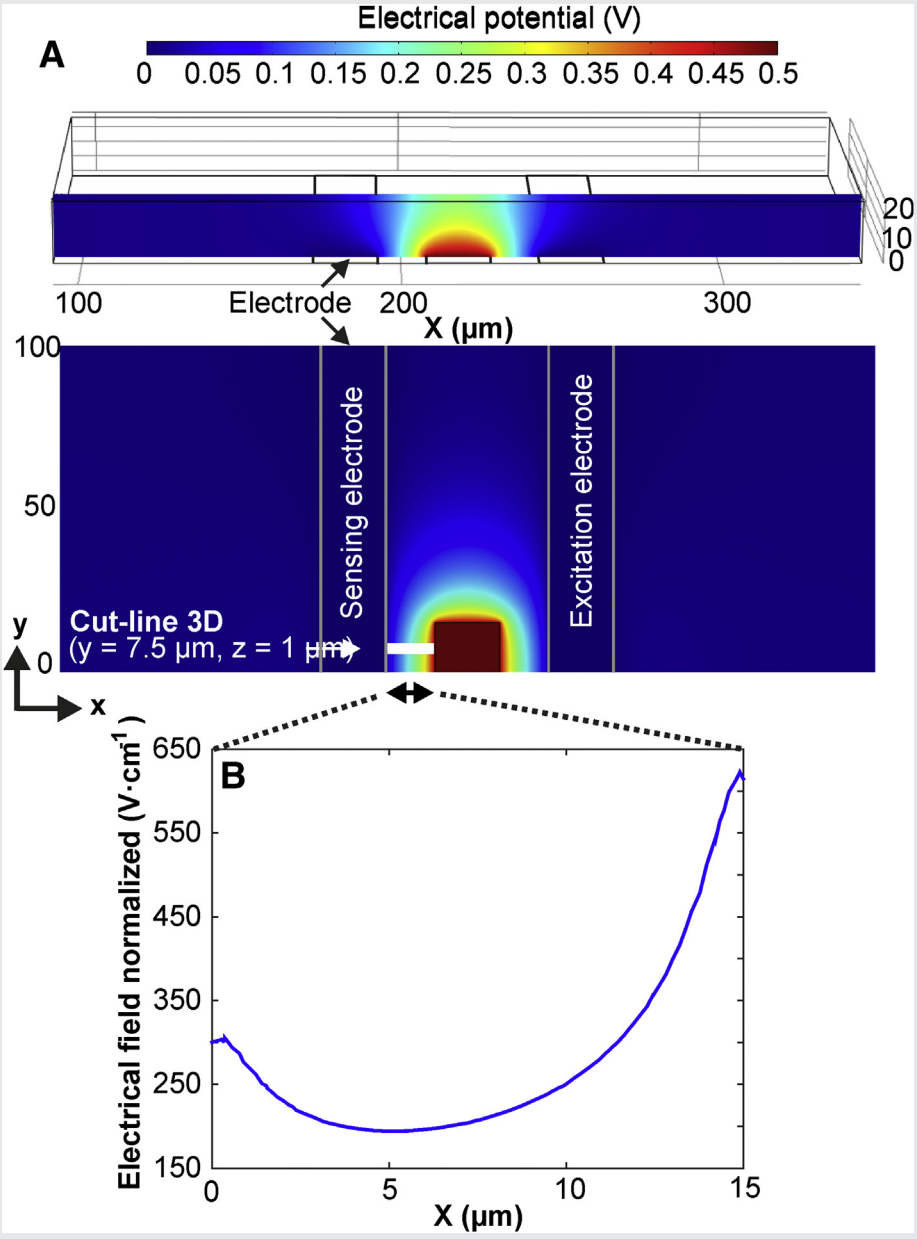

COMSOL simulation (v4.4) of the electrical field within the top channel of the microfluidic device. This simulation is based on a three-dimensional model (electrostatic), which described the electrical potential and normalized field strength under stationary conditions. (**A**) The orthogonal and top view of the field potential showed nonuniform behavior due to the nonsymmetrical electrode geometry. (**B**) A higher field strength was observed close to the excitation electrode compared with the sensing electrode when analyzing the field strength in the middle of the electrode array (y = 7.5 μm) at a height (z) of 1 μm.

de Wagenaar. Spermometer. Fertil Steril 2016.

SUPPLEMENTAL FIGURE 5

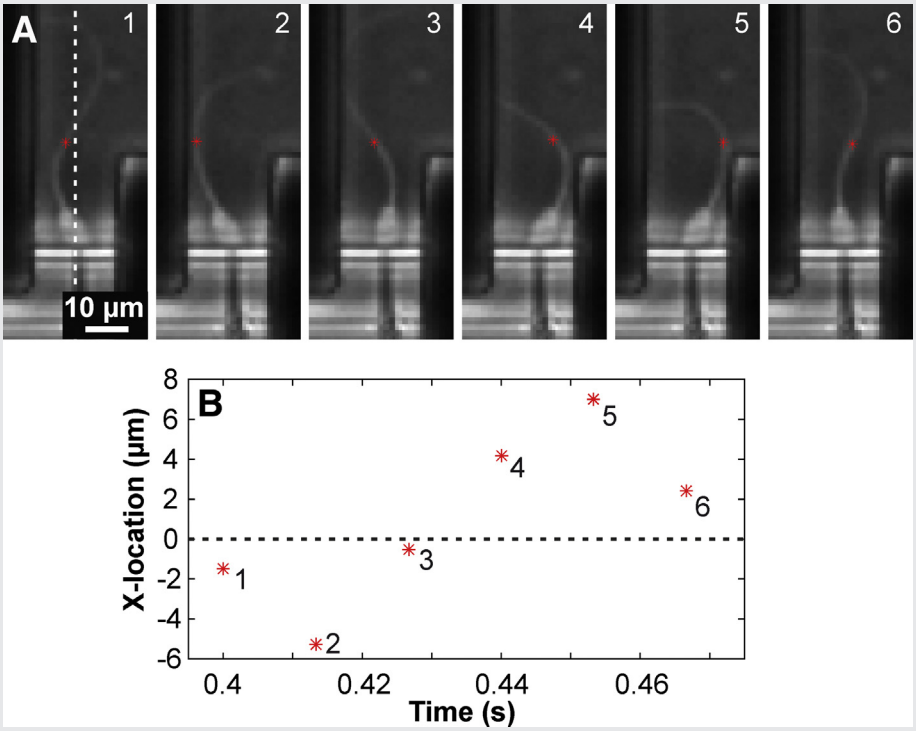

(**A**) Optical tracking of the sperm tail using a custom-built Matlab script. At each consecutive frame (at 75 fps) the sperm tail was tracked at a fixed distance with respect to the sperm trap and visualized with a *red asterisk*. The *white dashed line* indicates the center line, which is positioned at the center of the two electrodes. (**B**) The location of the tracked tail as a function of time. The *dashed line* is the center line, which is positioned at an X-location of 0 μm.

de Wagenaar. Spermometer. Fertil Steril 2016.

SUPPLEMENTAL FIGURE 6

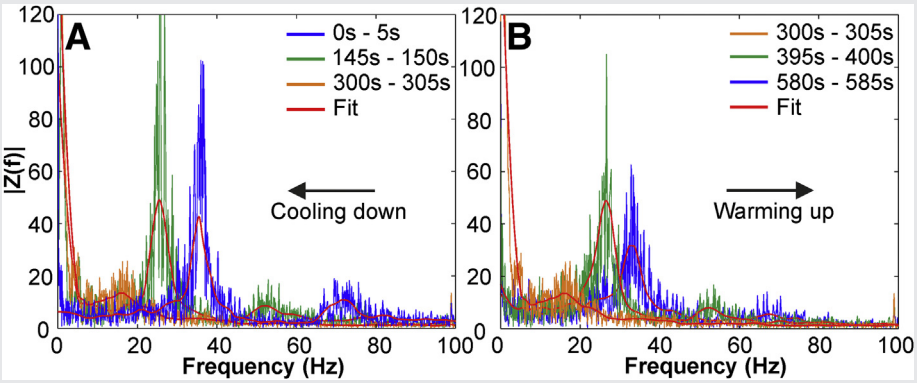

The effect of temperature on sperm beat frequency. Fast Fourier transform analysis was performed on the absolute impedance using 5-second intervals. (**A**) When the solution was cooling down, a decrease in base frequency was observed over time, which corresponds to the reduced flagellar beat frequency of the sperm cell due to the decrease in temperature. (**B**) Contrarily, the base frequency (i.e., beat frequency) was observed to increase over time when warming up the solution.

de Wagenaar. Spermometer. Fertil Steril 2016.